

COMMUNICATION




Cite this: *Phys. Chem. Chem. Phys.*,
2019, 21, 7256

Received 21st December 2018,
Accepted 28th January 2019

DOI: 10.1039/c8cp07786j

rsc.li/pccp

Surface-mediated spin dynamics probed by optical-pump–probe scanning tunneling microscopy†

Zi-Han Wang, Cheul-Hyun Yoon, Shoji Yoshida, Yusuke Arashida, Osamu Takeuchi, Yuzo Ohno and Hidemi Shigekawa *

In current materials science and technologies, surface effects on carrier and spin dynamics in functional materials and devices are of great importance. In this paper, we present the surface-sensitive probing of electron spin dynamics, performed by optical-pump–probe scanning tunneling microscopy (OPP–STM). Time-resolved spin lifetime information on a manganese (Mn)-deposited GaAs(110) surface was successfully obtained for the first time. With increasing Mn density via *in situ* evaporation, a nonlinear change in the spin lifetime in the picosecond range was clearly observed, while directly confirming the Mn density by STM. In comparison with the results obtained by the conventional OPP method, we have also demonstrated that the observed nonlinear spin lifetime behavior was surface-mediated, which can be characterized using only the surface-sensitive OPP–STM technique.

The use of functions realized in low dimensional materials such as topological insulators (TIs)¹ and mono-to-multi layer two-dimensional (2D) transition metal dichalcogenides (TMDCs)² has been attracting considerable attention. In particular, nano-scale spin dynamics and spin transport properties on surfaces and/or at interfaces are of great interest,^{3–6} and the application of their characteristics is being actively pursued^{7,8}. Therefore, a suitable measurement technique for the surface-sensitive characterization of spin-related properties with simultaneous high temporal and spatial resolutions is highly desirable. However, in conventional methods, information on spin-related properties is spatially averaged over a region including the bulk and generally is not surface-sensitive. For example, optical-pump–probe reflectivity (OPPR) has an excellent time resolution⁹ but its signal is generally averaged over the bulk in the light spot area. On the other hand, scanning tunneling microscopy (STM) is a promising technique to realize the investigation of the local electronic state while confirming atomic-level structures, and it has been

successfully used to investigate local electronic structures in TIs^{10,11} and various types of TMDCs.^{12,13} However, its time resolution has generally been limited to the millisecond or sub-millisecond range.^{14–16}

Recently, by combining the ultrafast OPP technique with STM, OPP–STM has been developed to obtain new insights into ultrafast dynamics at the nanoscale, which is far beyond the spatial resolution of conventional OPPR measurement while simultaneously surpassing the preamplifier-bandwidth-limited temporal resolution of conventional STM.¹⁷ Single-atomic-level measurement has been performed using this OPP–STM technique.^{18,19} Furthermore, the electron spin lifetime on GaAs and its nanostructures such as quantum wells, as well as spin precession dynamics under an external magnetic field,²⁰ has also been determined. Since OPP–STM probes the tunnel current, in addition to its high spatial resolution, high surface-sensitivity is also expected.

Here, we present the results of observing the electron spin dynamics on a manganese (Mn)-deposited GaAs (110) surface by OPP–STM as an example to demonstrate surface effects on spin dynamics. While confirming the structure of the surface, we attempted to reveal the effect of the surface impurities on the spin dynamics. In comparison with the results obtained by the conventional OPP method, we have demonstrated that the observed nonlinear spin lifetime behaviour was surface-mediated and can be characterized using only the surface-sensitive OPP–STM technique.

The experimental setup for OPPR and OPP–STM measurements is shown in Fig. 1. As is well known, the electron spin in semiconductors such as GaAs can be optically oriented by circularly polarized light.²¹ The OPP–STM system used in this work employs circularly polarized femtosecond laser pulses that couple to the STM tip–sample junction in a typical pump–probe scheme by using a novel laser polarization modulation technique while allowing the simultaneous observation of the surface by STM (see the ESI† for more details).

After confirming the quality of a GaAs(110) sample surface prepared by cleavage in a vacuum, Mn atoms were evaporated

Faculty of Pure and Applied Sciences, University of Tsukuba, Tsukuba, Ibaraki, 305-8573, Japan. E-mail: Hidemi@ims.tsukuba.ac.jp

† Electronic supplementary information (ESI) available. See DOI: 10.1039/c8cp07786j

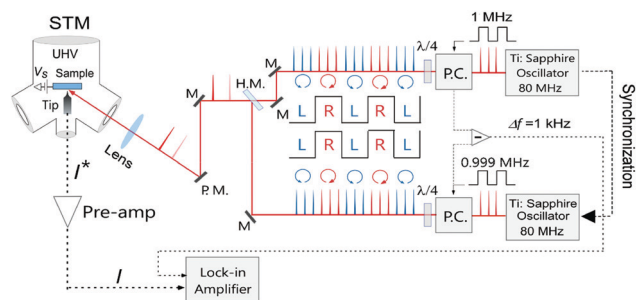


Fig. 1 Schematic illustration of the experimental setup. P.C.: ultrafast Pockels cells; M: mirror; H.M.: half mirror; P.M.: mirror on a piezo mirror mount; R: right-handed circularly polarized pulses, which correspond to the blue spikes and the blue circular arrows; L: left-handed circularly polarized pulses, which correspond to the red spikes and the red circular arrows. The polarization states (R or L) of laser pulses were modulated using Pockels cells, and aligned and steered using the necessary optics, and then the pulses were focused onto the sample surface in the UHV chamber. The slight frequency difference Δf in the modulation frequency $\Delta f = 1 \text{ MHz} - 0.999 \text{ MHz} = 1 \text{ kHz}$ here was used as the reference frequency for lock-in detection. The raw tunneling current I^* firstly amplified then lock-in-detected to obtain the time-resolved tunneling current signal as a function of the delay time t_d between the pump and probe pulses.

onto the surface at various deposition times, whose amounts were determined from STM images. Since Mn acts as an acceptor, it is possible to analyse the spin dynamics as compared with mechanisms such as electron–hole interactions.²² Two types of GaAs wafer were used: sample A to confirm the Mn densities on the surface prepared at different deposition times, and sample B for OPP-STM and OPPR experiments (see the ESI† for more details). Fig. 2(a)–(e) show typical STM images of sample A with different Mn densities. Fig. 2(f) shows the relationship between the evaporation time and the amount of

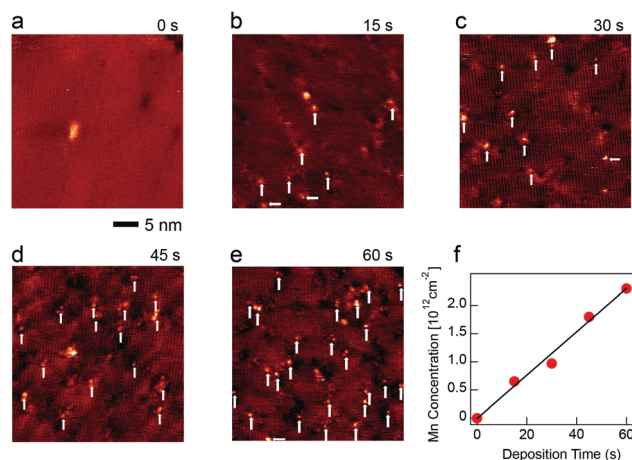


Fig. 2 Formation of Mn-deposited GaAs(110) surfaces. (a)–(e) Typical STM images of the GaAs(110) surfaces at different Mn deposition times ((a): clean, (b): 15 s, (c): 30 s, (d): 45 s, (e): 60 s) obtained using sample A. (f) Relationship between the deposition time and the amount of Mn atoms, which was determined by counting the number of Mn atoms, for example, indicated by the white arrows in (b) to (e), using wider STM images. A clear linear relationship was observed.

deposited Mn. The estimated Mn density on the surface linearly increased with the evaporation time as expected.

Next, OPP-STM measurements were carried out on Mn-deposited GaAs(110) surfaces. Sample B was cleaved in a vacuum and Mn was deposited on the surface by an identical procedure to that for sample A. Fig. 3(a) shows the spin signal intensity as a function of the delay time between the optical pump and probe pulses. The black lines are fitting curves with a single exponential function (see the ESI† for more details). Fig. 3(b) shows the spin lifetime determined by fitting as a function of the deposition time. Very interestingly, a nonlinear change in the spin lifetime was clearly observed. Namely, the spin lifetime increased until it reached a peak at a deposition time of 60 s, and then it started to decrease.

To understand the origin of the observed nonlinear spin lifetime behaviour, spin relaxation mechanisms are briefly reviewed. In n-type GaAs, as used in this experiment, at room temperature ($RT = 300 \text{ K}$), the dominant spin relaxation process is represented by the Dyakonov–Perel (DP) mechanism (see the ESI†, Fig. S1(a)).²³ Owing to the spin–orbit interaction, microscopic effective magnetic fields are generated and act upon

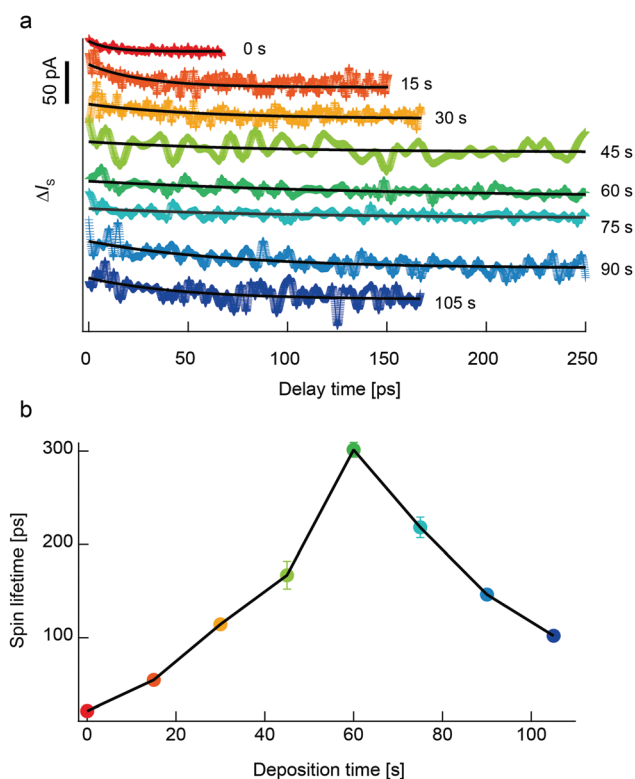


Fig. 3 Electron spin lifetime at different surface Mn densities obtained by OPP-STM. (a) Mn-density-dependent OPP-STM spectra, obtained for the samples shown in Fig. 2, in which the offset was manually adjusted for each spectrum. The black lines are fitting curves with a single exponential function, and the lifetimes determined were, from top to bottom, 21 ± 2 , 55 ± 3 , 114 ± 5 , 167 ± 15 , 301 ± 8 , 219 ± 11 , 146 ± 4 , and 102 ± 5 ps, respectively. (b) Spin lifetimes, which were determined from the fitting curves in (a), plotted as a function of the Mn deposition time. The peak lifetime was observed at a deposition time of 60 s, corresponding to a Mn density of $\sim 2.3 \times 10^{12} \text{ cm}^{-2}$. The same colors are used in (a) and (b).

electron spins, in which the impurity atoms included in the sample play an important role in determining the spin relaxation process. Namely, with spin-polarized electrons being scattered off by the impurities, spin relaxation occurs during two subsequent scattering events. Therefore, in the DP mechanism, the spin lifetime (τ_s) is inversely proportional to the momentum lifetime (τ_p), that is, $\tau_s \sim \tau_p^{-1}$. In contrast, in p-type GaAs at RT, particularly when the hole concentration is relatively high, the dominant process causing spin relaxation is the Bir-Aronov-Pikus (BAP) mechanism (see the ESI,† Fig. S1(b)),²³ in which the electrons lose their spin polarization owing to an ultrafast spin exchange interaction with the holes. In this case, the spin lifetime is inversely proportional to the hole density (n_h), *i.e.*, $\tau_s \sim n_h^{-1}$.

From the perspective described above, because the Mn atoms at 300 K act as paramagnetic impurities in the system, we found that the rate of scattering between the electrons and the Mn atoms, which suppresses the spin relaxation, increases with increasing Mn density, and the spin lifetime is initially extended owing to the DP mechanism. However, with a further increase in the surface Mn density, since most of the Mn atoms replace the Ga sites and act as acceptors,²⁴ effective (p-) doping on the surface induces a transition from a lightly doped n-type semiconductor to a hole-rich p-type one at and near the surface, and the decrease in the spin lifetime after it reached the peak position is attributed to the effect of the BAP mechanism. That is, at a relatively high surface Mn density, as the BAP mechanism is significantly enhanced, the increased competition between the DP and BAP mechanisms leads to an overall decrease in the spin lifetime. This effect of the DP-BAP competition upon increasing the effective p-type doping concentration has been theoretically predicted to occur in a similar p-type GaMnAs quantum well system.^{25,26} This is the first direct observation of the transition of the spin relaxation process from the DP mechanism to the BAP mechanism.

To evaluate the *z*-directional (perpendicular to the sample surface) spatial resolution of OPP-STM, conventional OPPR measurements were carried out on identical Mn-deposited surfaces using the same setup as that for OPP-STM with the STM tip extracted from the sample (see the ESI† for more details). Fig. 4(a) shows the OPPR signal as a function of the delay time. The black lines are fitting curves with a single exponential function. Fig. 4(b) shows the lifetimes determined from the data in Fig. 4(a), where the results obtained by OPP-STM presented in Fig. 3(b) are shown together for comparison. As is clearly shown, the tendency of the nonlinear lifetime observed by OPP-STM was much less pronounced in the case of OPPR measurement. This is considered to be due to the difference in the probing depth between OPP-STM and OPPR measurements.

In OPP-STM of a semiconductor, its signal mainly originates from the area where tip-induced band bending (TIBB) occurs.^{27,28} The spin-related tunnel current depends on the potential height determined by the amount of spin polarized photo-carriers excited by the pump and probe pulses, which depends on the delay time due to the mechanism of absorption bleaching. Namely, OPP-STM is highly sensitive to the surface dynamics. The TIBB

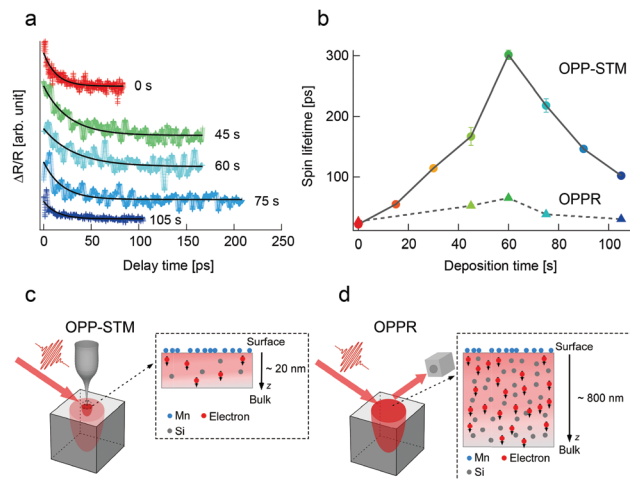


Fig. 4 Comparison of the spin lifetimes determined by the OPP-STM and OPPR methods. (a) Mn density dependent OPPR spectra. From top to bottom, the deposition time (Mn density) increased, with the offset manually adjusted for each spectrum. The black lines are fitting curves and the lifetimes determined were, from top to bottom, 26 ± 1 , 52 ± 1 , 65 ± 2 , 38 ± 1 , and 30 ± 1 ps, respectively. (b) Comparison of the deposition-rate dependence of the spin lifetime determined by the two methods. The results obtained by OPP-STM shown in Fig. 3b are shown together for comparison. (c) Schematic illustration of the probing area in OPP-STM measurement. (d) Schematic illustration of the probing area in OPPR measurement. The measured spin lifetime was almost entirely determined by the bulk, and the Mn-deposited surface had very little effect on the measured lifetime signal. Here, blue balls, Mn atoms; red balls, electrons; and grey balls, Si dopant atoms. For simplicity, only electrons with down spins are shown here.

depth is determined using parameters such as tip radius, tip-sample distance, bias voltage, and doping concentration. Considering the experimental conditions, as shown in Fig. 4(c), the effective depth was estimated to be over 10 nm (see the ESI,† Fig. S2). Whereas in OPPR measurement, the in-plane spatial resolution was determined using a laser spot size of 50 μm , and the spatial resolution perpendicular to the surface (*z*-direction) depends on the optical penetration depth, as shown in Fig. 4(d), which was ~ 800 nm in the present case (see the ESI,† Fig. S4) and much larger than that of OPP-STM. In the Mn-deposited GaAs(110) system, the Mn atoms existed only on the surface, acting as impurities and acceptors, and Mn ion diffusion to the bulk was suppressed during the OPP-STM measurement because the sample was reversely biased (positive sample bias). The influence of the screened Coulomb potential by Mn impurity is less than 10 nm.²⁹ Therefore, with increasing surface Mn density, the nonlinear spin lifetime behaviour, which was determined by both the DP and BAP mechanisms, is considered to only occur in the area close to the surface. In contrast, in the OPPR measurement, the time-resolved spin dynamics signal was obtained from deep inside the bulk, thus the nonlinear contribution from the surface was significantly reduced.

To further evaluate the observed difference between the two methods, we carried out simple simulations of spin excitation in OPP-STM measurement. That is, although our modulation

technique can probe only spin-related signals, the effect of the near field component should be suppressed to make band bending sensitive to spin-related absorption bleaching. In the case of a W tip, the tip-induced electric-field enhancement in the z-direction is about 400 times the incident light intensity, which sharply decreases inside the sample with increasing distance from the surface. Therefore, the circularly polarized light condition below the STM tip is initially disturbed around the tip apex but then quickly recovers at a depth of ~ 10 nm (see the ESI,† Fig. S3), which is comparable to the TIBB region, enabling the spin dynamics to be easily probed by OPP-STM. By adjusting the power of the incident laser, the depth where the circularly polarized light condition recovers may be controlled depending on the purpose. If one wants to observe the same nonlinear spin lifetime behaviour in a similar system such as GaMnAs using the conventional OPPR approach, several types of MBE-grown samples with different bulk Mn doping concentrations are necessary. That is, OPP-STM provides a powerful approach for studying electron spin dynamics, particularly when the surface and/or interface characteristics are of interest and have a deterministic role in the desired material functionalities. Combinations of OPP with low-temperature STM shows potential in further understanding nanoscale magnetism, the study of which is left as future work.

Conclusions

We have demonstrated that the dynamics of optically oriented spins in a Mn-deposited GaAs(110) surface can be probed by OPP-STM. With increasing Mn density *via in situ* evaporation, a nonlinear change in the electron-spin lifetime was clearly observed. Namely, the spin lifetime first increased and then decreased, with increasing density of Mn deposited on the surface. This characteristic can be comprehensively understood by considering the competition between two specific spin relaxation mechanisms, *i.e.*, the DP and BAP mechanisms. By comparing with results obtained by the conventional OPP method, we have also demonstrated that this nonlinear spin lifetime behaviour involved a surface-mediated modulation, which can be characterized exclusively by the OPP-STM technique. Further development and advancement of this technique, for example, combining with low-temperature STM, spin polarized STM,³⁰ multiprobe STM,³¹ and terahertz-coupled STM,^{32–34} is expected to be very promising in facilitating advances in the fields of nanoscience and nanotechnology.

Conflicts of interest

There are no conflicts to declare.

Acknowledgements

H. S. acknowledges the support from the Japan Society for the Promotion of Science (Grants-in-Aid for Scientific Research: 17H06088)

References

- 1 X. L. Qi and S. C. Zhang, *Rev. Mod. Phys.*, 2011, **83**, 1057.
- 2 W. Choi, N. Choudhary, G. H. Han, J. Park, D. Akinwande and Y. H. Lee, *Mater. Today*, 2017, **20**, 116.
- 3 H. Takeno, S. Saito and K. Mizuguchi, *Sci. Rep.*, 2018, **8**, 15392.
- 4 D. Hsieh, F. Mahmood, J. W. McIver, D. R. Gardner, Y. S. Lee and N. Gedik, *Phys. Rev. Lett.*, 2011, **107**, 077401.
- 5 L. Yang, W. Chen, K. M. McCreary, B. T. Jonker, J. Lou and S. A. Crooker, *Nano Lett.*, 2015, **15**, 8250.
- 6 Y. K. Luo, J. Xu, T. Zhu, G. Wu, E. J. McCormick, W. Zhan, M. R. Neupane and R. K. Kawakami, *Nano Lett.*, 2017, **17**, 3877.
- 7 J. Tian, I. Childres, H. Gao, T. Shen, I. Miotkowski and Y. P. Chen, *Solid State Commun.*, 2014, **191**, 1.
- 8 W. Han, *APL Mater.*, 2016, **4**, 032401.
- 9 R. P. Prasankumar and A. J. Taylor, *Optical Techniques for Solid State Materials Characterization*, CRC Press, 1st edn, 2011.
- 10 Z. Alpichshev, J. G. Analytis, J. H. Chu, I. R. Fisher, Y. L. Chen, Z. X. Shen, A. Fang and A. Kapitulnik, *Phys. Rev. Lett.*, 2010, **104**, 016401.
- 11 Y. Zhang, K. He, C. Z. Chang, C. L. Song, L. L. Wang, X. Chen, J. F. Jia, Z. Fang, X. Dai, W. Y. Shan, S. Q. Shen, Q. Niu, X. L. Qi, S. C. Zhang, X. C. Ma and Q. K. Xue, *Nat. Phys.*, 2010, **6**, 584.
- 12 S. Yoshida, Y. Kobayashi, R. Sakurada, S. Mori, Y. Miyata, H. Mogi, T. Koyama, O. Takeuchi and H. Shigekawa, *Sci. Rep.*, 2015, **5**, 14808.
- 13 C. Zhang, M. Y. Li, J. Tersoff, Y. Han, Y. Su, L. J. Li, D. A. Muller and C. K. Shih, *Nat. Nanotechnol.*, 2018, **13**, 152.
- 14 H. J. Mamin, H. Birk, P. Wimmer and D. Rugar, *J. Appl. Phys.*, 1994, **75**, 161.
- 15 J. Wintterlin, J. Trost, S. Renisch, R. Schuster, T. Zambelli and G. Ertl, *Surf. Sci.*, 1997, **394**, 159.
- 16 U. Kemiktarak, T. Ndikum, K. C. Schwab and K. L. Ekinci, *Nature*, 2007, **450**, 85.
- 17 M. Yamashita, H. Shigekawa and R. Morita, *Monocycle Photonics and Optical Scanning Tunneling Microscopy: Springer Series in Optical Sciences 99*, Springer, 2005.
- 18 Y. Terada, S. Yoshida, O. Takeuchi and H. Shigekawa, *Nat. Photonics*, 2010, **12**, 869.
- 19 S. Yoshida, M. Yokota, O. Takeuchi, H. Oigawa, Y. Mera and H. Shigekawa, *Appl. Phys. Express*, 2013, **6**, 032401.
- 20 S. Yoshida, Y. Aizawa, Z. H. Wang, R. Oshima, Y. Mera, E. Matsuyama, H. Oigawa, O. Takeuchi and H. Shigekawa, *Nat. Nanotechnol.*, 2014, **9**, 588.
- 21 F. Meier and B. P. Zakharchenya, *Optical Orientation: Vol. 8 of Modern Problems in Condensed Matter Sciences*, Elsevier, 1st edn, 1984.
- 22 J. H. Jiang, Y. Zhou, T. Korn, C. Schuller and M. W. Wu, *Phys. Rev. B: Condens. Matter Mater. Phys.*, 2009, **79**, 155201.
- 23 M. I. Dyakonov, *Spin Dynamics in Semiconductors: Springer Series in Solid-State Sciences 157*, Springer, 2008.
- 24 A. Taninaka, S. Yoshida, K. Kanazawa, E. Hayaki, O. Takeuchi and H. Shigekawa, *Nanoscale*, 2016, **8**, 12118.

- 25 J. H. Jiang, Y. Zhou, T. Korn, C. Schuller and M. W. Wu, *Phys. Rev. B: Condens. Matter Mater. Phys.*, 2009, **79**, 155201.
- 26 M. W. Wu, J. H. Jiang and M. Q. Weng, *Phys. Rep.*, 2010, **493**, 61.
- 27 S. Yoshida, Y. Terada, M. Yokota, O. Takeuchi, H. Oigawa and H. Shigekawa, *Eur. Phys. J.: Spec. Top.*, 2013, **222**, 1161.
- 28 M. Yokota, S. Yoshida, Y. Mera, O. Takeuchi, H. Oigawa and H. Shigekawa, *Nanoscale*, 2013, **5**, 9170.
- 29 S. Yoshida, Y. Kanitani, O. Takeuchi and H. Shigekawa, *Appl. Phys. Lett.*, 2008, **92**, 102.
- 30 R. Wiesendanger, *Rev. Mod. Phys.*, 2009, **81**, 1495.
- 31 T. Nakayama, O. Kubo, Y. Shingaya, S. Higuchi, T. Hasegawa, C. S. Jiang, T. Okuda, Y. Kuwahara, K. Takami and M. Aono, *Adv. Mater.*, 2012, **24**, 1675.
- 32 T. L. Cocker, D. Peller, P. Yu, J. Repp and R. Huber, *Nature*, 2016, **539**, 263.
- 33 K. Yoshioka, I. Katayama, Y. Minami, M. Kitajima, S. Yoshida, H. Shigekawa and J. Takeda, *Nat. Photonics*, 2016, **10**, 762.
- 34 V. Jelic, K. Iwaszczuk, P. H. Nguyen, C. Rathje, G. J. Hornig, H. M. Sharum, J. R. Hoffman, M. R. Freeman and F. A. Hegmann, *Nat. Phys.*, 2017, **13**, 591.